

Thermal and suction effects on the anisotropic elastic shear moduli under various stress conditions

Obed Takyi BENTIL^{1,*}, Chao ZHOU²

¹Department of Civil and Environmental Engineering, The Hong Kong Polytechnic University, Hung Hom, Hong Kong;
o-t.bentil@connect.polyu.hk

²Department of Civil and Environmental Engineering, The Hong Kong Polytechnic University, Hung Hom, Hong Kong;
c.zhou@polyu.edu.hk

*Correspondence: o-t.bentil@connect.polyu.hk

SUBMITTED 27 November 2024 REVISED 25 December 2024 ACCEPTED 29 April 2025

ABSTRACT The elastic shear modulus of soils plays a pivotal role in assessing the serviceability of various geotechnical engineering infrastructures, particularly those subjected to fluctuating temperatures and suction levels. Despite its significance, the combined influence of temperature and suction on the elastic shear modulus remains inadequately explored. This study endeavours to improve the understanding of temperature and suction-dependent elastic shear modulus by employing an oedometer and an advanced triaxial apparatus capable of controlling temperature and suction, integrated with bender element probes and local strain measurement techniques. The investigation focuses on the anisotropic behaviour of the elastic modulus across a temperature range of 5 to 40 °C and suction values between 0 and 300 kPa under both saturated and unsaturated conditions. At the same temperature, the elastic shear modulus increases with an increase in suction, which is mainly attributed to stiffening effects of water meniscus with increasing suction. The results consistently indicate a decrease in the shear modulus after heating for all stress levels and suction conditions investigated. This heating-induced reduction can be attributed to several factors, including the reduction of interparticle forces and the decrease in air-water surface tension due to heating. Furthermore, the extent of the reduction in shear modulus depends upon the orientation of the shear plane, highlighting a significant change in the degree of anisotropy post-heating. This study sheds light on the complex interplay between temperature, suction, and the elastic shear modulus of soils and underscores the necessity for incorporating these coupled effects into the design and analysis of geotechnical structures under varying environmental conditions.

KEYWORDS

Temperature; suction; anisotropy; elastic shear modulus; clayey soil

1 INTRODUCTION

Soils around geothermal engineering structures, such as energy piles and tunnels, experience temperatures. These soils are frequently unsaturated and experience different levels of suction or negative pore water pressures. The combined effects of suction and temperature on the mechanical behaviour of soils can be quite complex. As revealed in the literature, suction affects the volume, shear strength, and stiffness of unsaturated soil (Han and Vanapalli, 2016, Ng and Yung, 2008, Ng et al., 2009). On the other hand, temperature variations can cause volumetric changes, affect pore water pressure and water content, and induce thermal stresses (Cai et al., 2023, Cai et al., 2011, Alsherif and McCartney, 2015, Alsherif and McCartney, 2016). Since temperature changes can alter soil suction at constant water content or induce changes in water content at constant suction, when suction and temperature interact, they can lead to significant alterations in soil behaviour. These coupled effects can lead to changes in the soil's mechanical behaviour, such as stiffness, shear strength, and compressibility, as revealed in the literature (Ng and Zhou, 2014, Thota and Vahedifard, 2021, Uchaipichat and Khalili, 2009, Vahedifard et al., 2020, Cai et al., 2023).

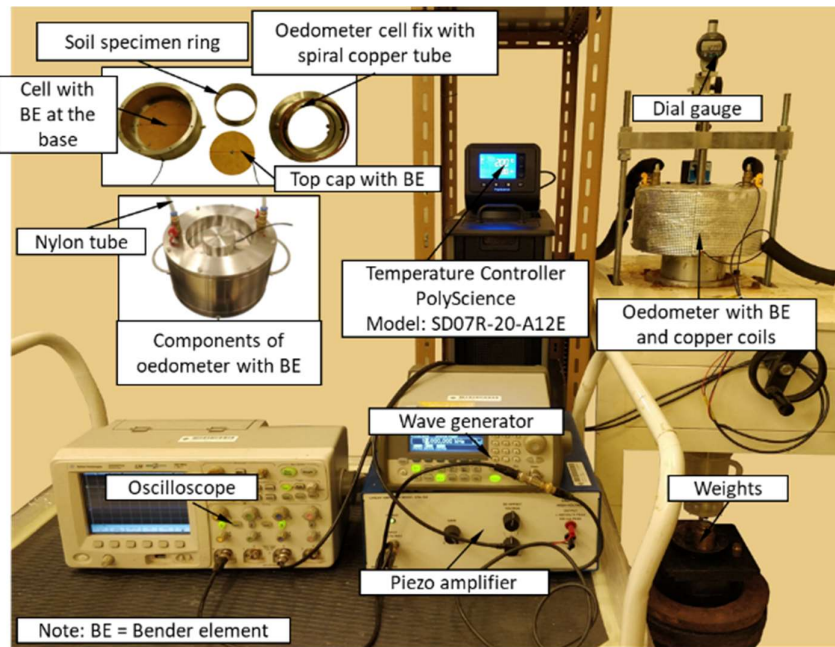
Understanding these coupled effects is essential for geotechnical engineers and researchers, particularly in environments where both suction and temperature variations are significant. This knowledge helps predict the soil's mechanical responses under coupled suction-temperature conditions, ensuring the safety and stability of geotechnical systems. So far, many researchers have investigated the temperature effects on yield stress and shear strength, which is related to thermo-plasticity. To gain an improved insight on the temperature effects on soil behaviour, it is relevant to investigate the influence of temperature on the elastic shear modulus $G_{0(ij)}$ of soil on the shear plane ij . $G_{0(ij)}$ may be anisotropic due to the specimen preparation method and the mode of soil formation (e.g., Jovičić and Coop, 1998) and when estimating ground movements for designing the serviceability of geostructures $G_{0(ij)}$ is crucial parameter (Cai et al., 2015). Vahedifard et al. (2020) determined $G_{0(vh)}$ of unsaturated silt by employing bender elements in a temperature-controlled triaxial and discovered that $G_{0(vh)}$ decreased as soil is heated from 23°C to 43 °C. In addition, the thermal effects on $G_{0(vh)}$ were found to be more pronounced at higher suctions. Davoodi-Bilesavar and Hoyos (2023) studied the thermal effects on $G_{0(vh)}$ of three saturated soils using a temperature-controlled resonant column system. They also reported that increasing temperature reduces the elastic shear moduli.

Results from the above studies are valuable for understanding the thermal effects on $G_{0(ij)}$. However, more data are needed to comprehend the coupled effects of suction and temperature on $G_{0(ij)}$ of soils, which is very relevant to energy geostructures in dry and semi-arid regions. More importantly, all of the previous studies measured $G_{0(ij)}$ in a single shear plane, and experiments are needed to understand the influence of suction and temperature on the degree of stiffness anisotropy. In this study, a temperature-controlled oedometer and triaxial devices with bender element probes were developed. Using these apparatuses, a compacted clayey soil was tested to investigate thermal effects on the anisotropic elastic shear $G_{0(ij)}$ of soil specimens at various suctions. The coupled effects of temperature and suction are analysed in detail.

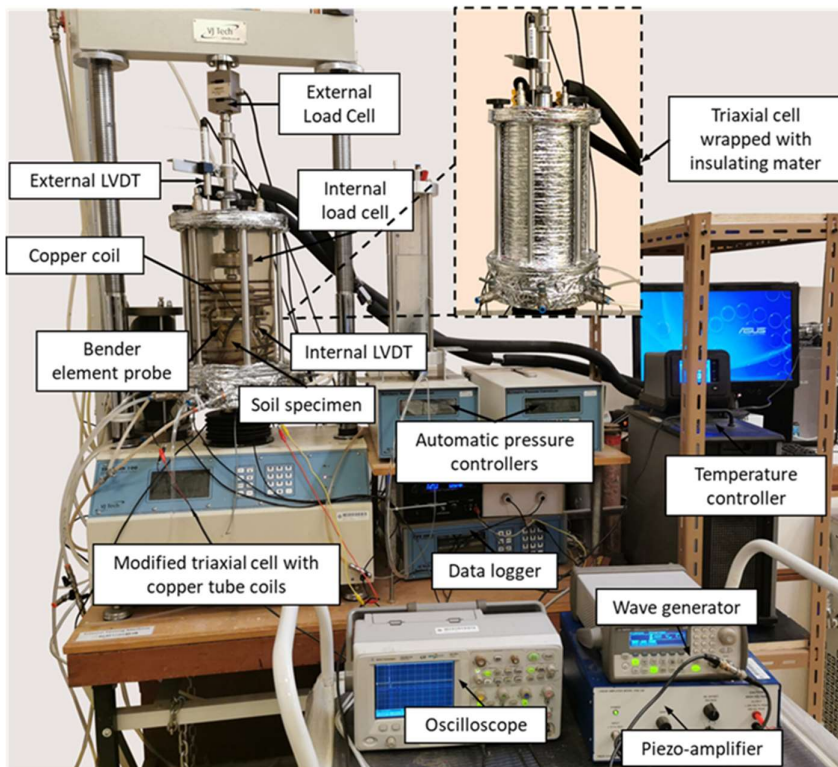
2 METHODS

2.1 Test Apparatuses

One-dimensional compression tests were conducted using a temperature-controlled oedometer equipped, as shown in Figure 1(a). Isotropic compression tests were conducted with a suction and temperature-controlled triaxial apparatus equipped local strain measurements, as shown in Figure 1(b). Both apparatuses are equipped with shear wave velocity measurement system using bender elements. In both devices, heated or cooled water from a temperature control system was circulated around the soil sample in a spiral copper coil to regulate the soil's temperature. During testing, an insulating covering was utilized to wrap these devices to reduce heat loss. A thermocouple was installed within the apparatuses close to the test specimen to monitor soil temperature. A pair of bender elements were installed in the oedometer to measure the travel time of shear wave propagation, estimate the shear wave velocity, $v_{(vh)}$ and then calculate the $G_{0(vh)}$ of the soil specimen, whereas two pairs of bender elements were used to measure the travel time of shear wave propagation, estimate the anisotropic shear wave velocities, $v_{(hh)}$ and $v_{(hv)}$, and then calculate the anisotropic elastic shear modulus, $G_{0(hh)}$ and $G_{0(hv)}$. In this study, the peak-to-peak method was used to deduce the travel time for the arrival of shear wave because of its simplicity. According to a number of calibration tests, the bender element system performed well at temperatures ranging from 5 to 60 °C. As a result, all tests were conducted between 5 and 60 °C.



(a)



(b)

Figure 1 Temperature-controlled apparatuses equipped with shear wave velocity measurements (a) oedometer for saturated tests (b) triaxial for both saturated and unsaturated tests

2.2 Test Soil

A lateritic clay, which has a fraction of sand, silt and clay of 42%, 30% and 28%, respectively was used in this study. Its liquid limit 47% and plastic limit is 26%. It is classified as sandy lean clay (CL) with reference to the USCS (ASTM, 2017). More information on this soil can be found in Ng et al. (2019). The specimens were statically compacted under a target moisture content of 19.5% which is the optimum moisture content (OMC). The dry density was 1.62 g/cm³, corresponding to 95% of the maximum dry density (MDD) determined by the standard proctor compaction.

2.3 Test Program and Procedures

To study the effects of temperature and stress on $G_{0(vh)}$, a series of tests summarized in Table 1 was designed. A cyclic heating-cooling test with a temperature ranging from 5 to 60 °C was carried out at 50 and 400 kPa vertical stress with the thermo-mechanical path shown in Figure 2 using the oedometer apparatus. The specimens were compressed to the pre-defined stress (i.e., O-A and O-B, respectively) at 20°C and then progressively heated and cooled (i.e., A-A₁-A₂ and B-B₁-B₂ for each cycle, respectively) considering temperatures of 5, 20, 30, 40, 50 and 60 °C. To ensure that the soil attained thermal equilibrium, each temperature was held for 12 hours. During this period, the vertical deformation of the soil was monitored using a dial gauge. Shear wave velocity measurements were obtained to calculate $G_{0(vh)}$ at the intended thermo-mechanical states shown by pointers in Figure 2.

Table 1 Test program for thermal cycles on $G_{0(vh)}$ at constant one-dimensional stress

Test ID	Effective vertical stress, σ'_v : kPa	Suction, s : kPa	Stress path
σ'_v 50	50	0	O-A-A ₁ -A ₂ *
σ'_v 400	400	0	O-B-B ₁ -B ₂ *

Note: *At each stress condition, a thermal cycle was applied to the specimen with the following stages: 20 → 5 → 20 → 30 → 40 → 50 → 60 → 5 °C.

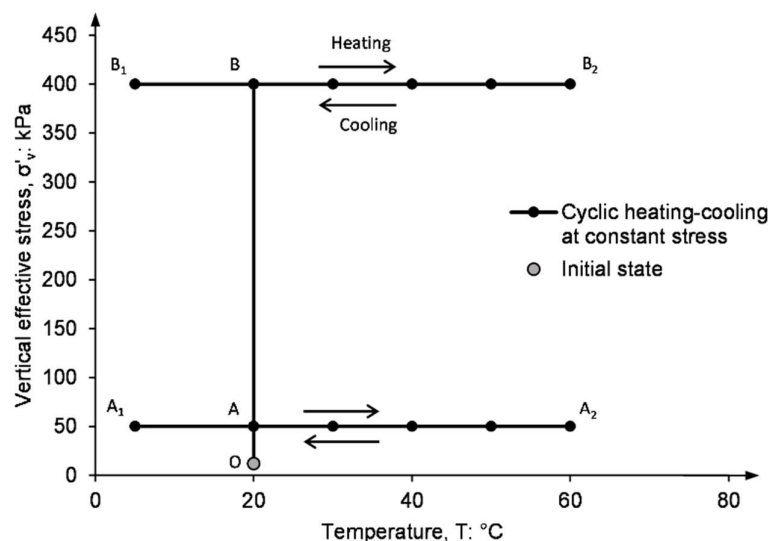


Figure 2 Thermo-mechanical paths for cyclic heating-cooling at constant 1D stress in oedometer apparatus

A series of tests was designed to study the coupled effects of suction and temperature on $G_{0(ij)}$, as summarized in Table 2. Three suctions (i.e., 0, 150 and 300 kPa) and two mean net stresses (i.e., 50 and 200 kPa) were considered. Figure 3 shows the thermo-hydro-mechanical stress path of all test specimens in the triaxial apparatus. The compacted specimens have an initial suction of about 150 kPa. The initial conditions of the specimens are denoted by A, as shown in Figure 2(b). Each test consists of three stages: isotropic compression, suction equalisation and cyclic heating-cooling. First of all, the specimen was compressed isotropically to the predefined mean net stress (i.e., 50 or 200 kPa) at constant water content by closing the water drainage valve in the apparatus and room temperature of 20 °C. Then, the specimen was subjected to the target suction, with equalisation criteria of daily gravimetric water content change of less than 0.09% (Chiu and Ng, 2012), generally taking 7 to 14 days. After suction equalisation, which generally took about 14 days, soil temperature was changed stepwise: 20→5→20→40→20 °C. Each temperature was maintained for 24 hours, enough for thermal equilibrium in the unsaturated soil. The bender element test was conducted after thermal equalisation to estimate the anisotropic shear wave velocity and calculate the anisotropic elastic shear modulus, $G_{0(hh)}$ and $G_{0(hv)}$. After the thermal cycle at zero suction, the specimen was dried to a suction of 150 kPa. The drying process was achieved by reducing the pore water pressure value to a target value in order to obtain the desired soil suction. After suction equalization, one thermal cycle described above was applied to the specimen. Similar procedures were used for a suction value of 300 kPa. Note that one specimen was used for the testing at three different suctions. The advantages include fewer soil specimens being tested, less laboratory time consumption and reduced effects of heterogeneity among the specimens. This methodology is similar to a multistage loading trend and was utilized in other studies (e.g., Davoodi-Bilesavar and Hoyos, 2023).

Table 2 Test program for the coupled suction and thermal effects on $G_{0(ij)}$.

Test ID	Mean net stress, p : kPa	Suction, s : kPa	Stress path
p50 s0	50	0	A-B ₁ -C ₁ *
p200 s0	200	0	A-B ₂ -C ₂ *
p200 s150		150	A-B ₂ -D ₂ *
p200 s300		300	A-B ₂ -E ₂ *

Note: *At each suction condition, a thermal cycle was applied to the specimen with the following stages: 20 → 5 → 20 → 40 → 20°C.

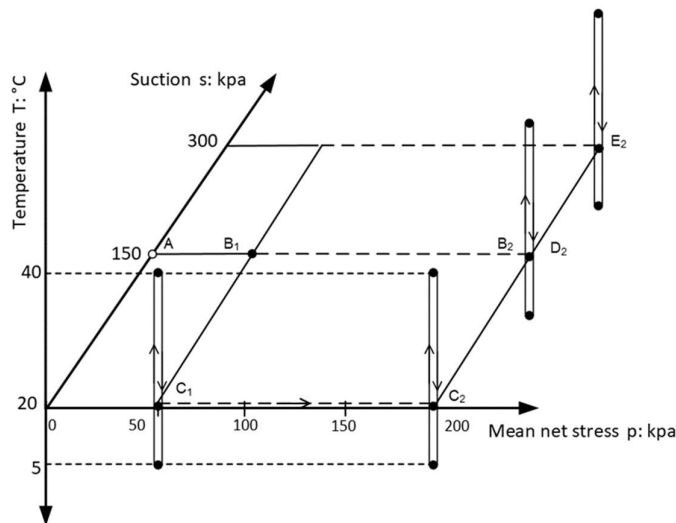


Figure 3 Thermo-hydro-mechanical paths cyclic heating at constant suction and constant isotropic mean net stress in triaxial apparatus

3 RESULTS

3.1 Effects of temperature cycle on shear moduli at various suction and stress conditions

Figure 4(a) shows $G_{0(vh)}$ measured during a single thermal cycle at a vertical effective stress of 400 kPa. The value of $G_{0(vh)}$ reduces during heating while it increases during cooling. On the other hand, Figure 4(b) shows the values $G_{0(vh)}$ during the heating-cooling cycle at vertical effective stress of 50 kPa, whose trend is similar to that at 400 kPa. The $G_{0(vh)}$ of the clay increased after one heating-cooling cycle, as revealed in Figure 4, and this result is primarily attributed to cyclic heating/cooling inducing soil densification caused by volumetric contraction. For the vertical effective stresses of 400 and 50 kPa, $G_{0(vh)}$ increased by roughly 10% and 2% after one heating-cooling cycle, respectively. Perhaps the reason for this difference is that the contractive strain was significantly higher at 400 kPa.

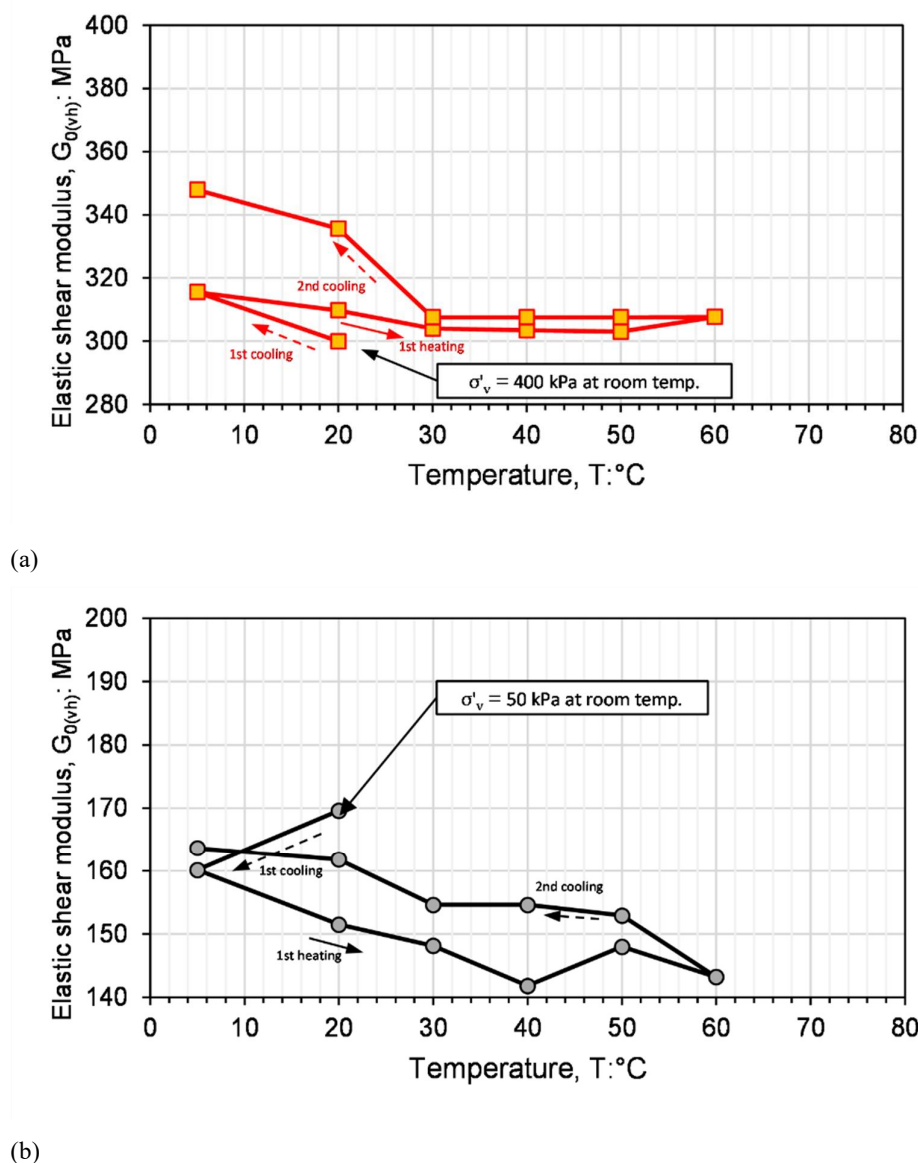
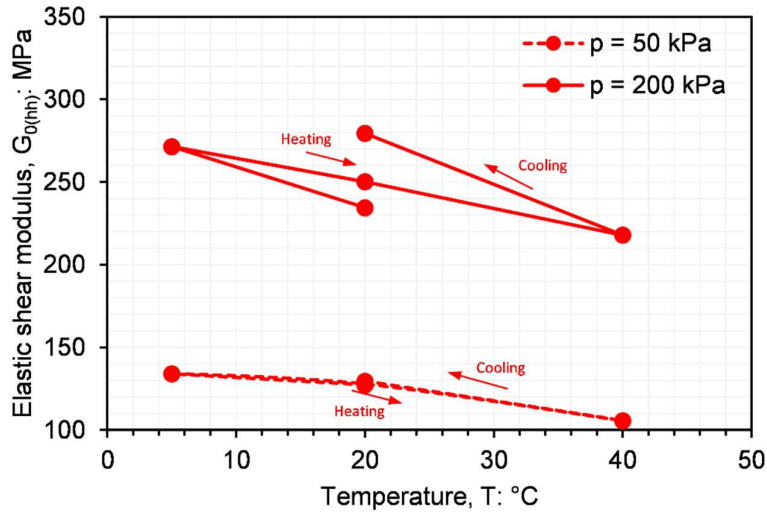


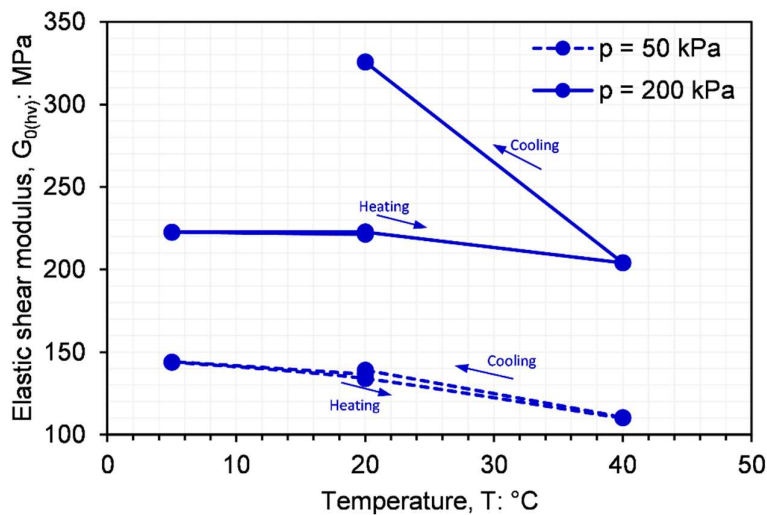
Figure 4 Variation in stiffness at vertical effective stresses of (a) 400 kPa and (b) 50 kPa after cyclic heating and cooling.

3.2 Effects of thermal cycle on stiffness under isotropic stress conditions

Figure 5 shows the thermally induced variations of $G_{0(ij)}$ under zero suction and mean net stresses of 50 and 200 kPa. Generally, $G_{0(ij)}$ reduces as the soil temperature increases, and discussion is given later. Moreover, $G_{0(ij)}$ increases after one thermal cycle, similar to the results under 1D stress conditions presented earlier. This is likely attributed to the overall volumetric contractive causing densification during the thermal cycle, leading to increased particle contacts.



(a)

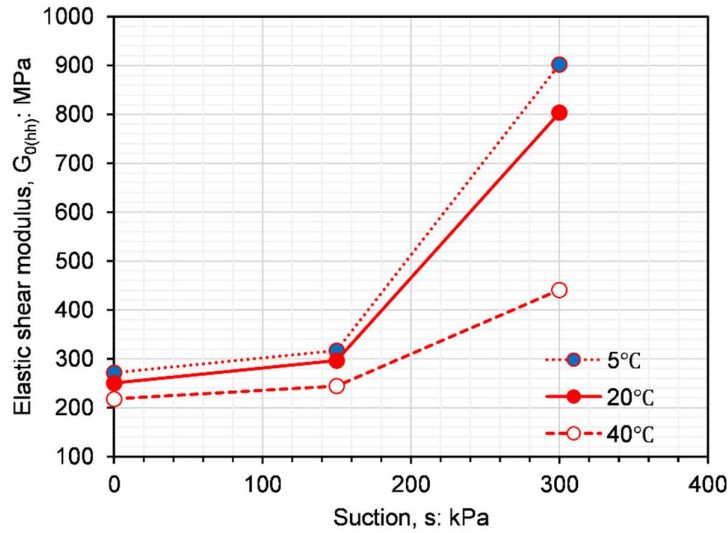


(b)

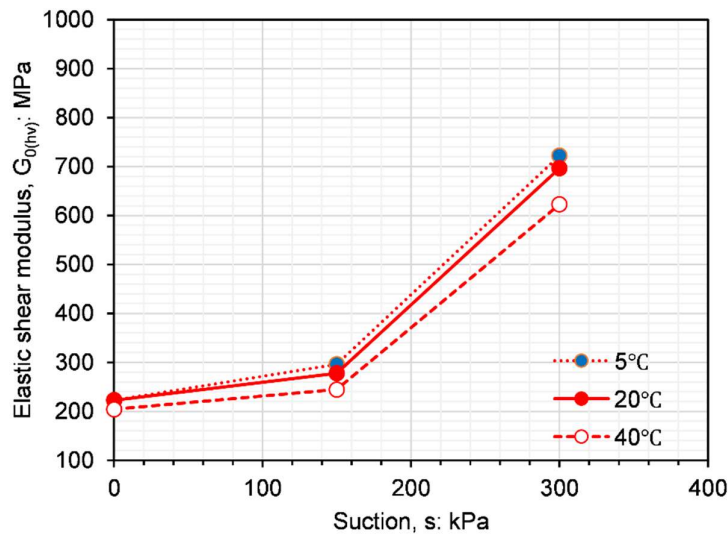
Figure 5 Effects of thermal cycle on stiffness at under isotropic mean net stress for (a) $G_{0(hh)}$ and (b) $G_{0(hv)}$

3.3 Suction effects on stiffness at different temperatures

Figure 6 represents the $G_{0(ij)}$ variation with suction at 200 kPa net mean stress and three different temperatures of 5, 20 and 40°C. As expected, an increase in suction increases both $G_{0(hh)}$ and $G_{0(hv)}$, irrespective of the temperature. The stiffening effects of water meniscus (Heitor et al., 2013, Mancuso et al., 2002, Ng and Xu, 2012, Ng and Yung, 2008, Sawangsuriya et al., 2009) or an increase in Bishop's effective stress with increasing suction is the main reason this trend. Moreover, the difference in $G_{0(ij)}$ at 5 and 40°C becomes larger as suction increases. Similar findings were obtained by Vahedifard et al. (2020) based on the measurement of $G_{0(ij)}$ at a single shear plane.



(a)



(b)

Figure 6 Suction effects on the (a) $G_{0(hh)}$ and (b) $G_{0(hv)}$ at different temperatures and mean net stress of 200 kPa.

4 DISCUSSION

Both one-dimensional stress conditions from the temperature-controlled oedometer and isotropic stress conditions from the temperature-controlled triaxial apparatus revealed that the $G_{0(ij)}$ generally decreases during heating and increases during cooling. The results can be attributed to temperature effects on the interparticle force of saturated clay (Laloui, 2001). In the double layer theories (Israelachvili, 2011), increasing soil temperature would increase the electrical repulsive force between soil particles. The increase in the electrical repulsive forces causes a reduction of $G_{0(ij)}$. At unsaturated conditions, the presence of water meniscus (Gallipoli et al., 2003, Lourenço et al., 2012, Wheeler and Karube, 1996) can stabilise the soil. However, at a constant suction condition, an increase in temperature reduces the surface tension of the air-water interfaces, weakening the contributions of the water menisci, causing a potential decrease of the degree of saturation and hence the reduction of Bishop's effective stress (Bentil et al., 2024). This reduction can further decrease the $G_{0(ij)}$ during heating.

5 CONCLUSION

This study set out to determine thermal effects on anisotropic shear modulus $G_{0(ij)}$ of saturated and unsaturated clayey soil using an oedometer and triaxial devices equipped with shear wave velocity measuring instruments. At a constant temperature, an increase in suction results in an increase in $G_{0(ij)}$. This is mainly attributed to stiffening effects of water meniscus, an increase in average skeleton stress or Bishop's effective stress with increasing suction for the suction range in this study. At the same suction, $G_{0(ij)}$ is lower at a higher temperature. This is likely because an increase in temperature causes an increase in the repulsive electric forces between particle contacts of fine-grained soils. Another possible explanation for this is that with increasing temperature at constant suction, there is a reduction in the air-water surface tension between particles and aggregates. Moreover, there is a tendency for $G_{0(ij)}$ to increase after cyclic heating and cooling. Soil contraction and particle rearrangement brought on by heating-cooling cycles are primarily responsible for this increase. These aforementioned findings offer empirical data to improve the modelling of thermo-elasticity in constitutive models and the analysis of thermally operational geo-structures.

DISCLAIMER

The authors declare no conflict of interest.

AVAILABILITY OF DATA AND MATERIALS

All data are available from the author.

ACKNOWLEDGMENTS

The authors also would like to thank the Research Grants Council (RGC) of the HKSAR for providing financial support through the grants N_PolyU526/23 and 15200120.

REFERENCES

- Alsherif, N.A. & McCartney, J.S., 2015. Thermal behaviour of unsaturated silt at high suction magnitudes. *Géotechnique*, 65, pp. 703-716. <https://doi.org/10.1680/geot.14.P.049>
- Alsherif, N.A. & McCartney, J.S., 2016. Yielding of Silt at High Temperature and Suction Magnitudes. *Geotechnical and Geological Engineering*, 34, pp. 501-514. <https://doi.org/10.1007/s10706-015-9961-x>
- ASTM, 2017. D2487 – 17e1: Standard Practice for Classification of Soils for Engineering Purposes (Unified Soil Classification System). West Conshohocken, Pa. USA: ASTM International.
- Bentil, O.T., Liu, K. & Zhou, C., 2024. Coupled effects of temperature and suction on the anisotropic elastic shear moduli of unsaturated soil. *Canadian Geotechnical Journal*, 62, pp. 1-8. <https://doi.org/10.1139/cgj-2023-0757>
- Cai, G., Liu, Y., Liu, Z., Zhou, A., Li, J. & Zhao, C., 2023. Volume change behaviour of an unsaturated compacted loess under thermo-hydro-mechanical loads. *Acta Geotechnica*, 19, pp. 2023-2040. <https://doi.org/10.1007/s11440-023-01995-1>
- Cai, G., Zhao, C., Liu, Y. & Li, J., 2011. Volume change behavior of unsaturated soils under non-isothermal conditions. *Chinese Science Bulletin*, 56, pp. 2495-2504. <https://doi.org/10.1007/s11434-011-4580-2>
- Cai, Y., Sanghaleh, A. & Pan, E., 2015. Effect of anisotropic base/interlayer on the mechanistic responses of layered pavements. *Computers and Geotechnics*, 65, pp. 250-257. <https://doi.org/10.1016/j.compgeo.2014.12.014>

- Chiu, C.F. & Ng, C.W.W., 2012. Coupled water retention and shrinkage properties of a compacted silt under isotropic and deviatoric stress paths. *Canadian Geotechnical Journal*, 49, pp. 928-938. <https://doi.org/10.1139/t2012-055>
- Davoodi-Bilesavar, R. & Hoyos, L.R., 2023. Small-Strain Stiffness of Cohesive-Frictional Soils from Thermo-controlled Constant Water Content Resonant Column Testing. *Geotechnical Testing Journal*, 46, pp. 651-674. <https://doi.org/10.1520/GTJ20220197>
- Gallipoli, D., Gens, A., Sharma, R. & Vaunat, J., 2003. An elasto-plastic model for unsaturated soil incorporating the effects of suction and degree of saturation on mechanical behaviour. *Géotechnique*, 53, pp. 123-136. <https://doi.org/10.1680/geot.2003.53.1.123>
- Han, Z. & Vanapalli, S.K., 2016. Stiffness and shear strength of unsaturated soils in relation to soil-water characteristic curve. *Géotechnique*, 66, pp. 627-647. <https://doi.org/10.1680/jgeot.15.P.104>
- Heitor, A., Indraratna, B. & Rujikiatkamjorn, C., 2013. Laboratory study of small-strain behavior of a compacted silty sand. *Canadian Geotechnical Journal*, 50, pp. 179-188. <https://doi.org/10.1139/cgj-2012-0037>
- Israelachvili, J., 2011. *Intermolecular and surface forces*. 3rd ed. New York: 3rd Edition. Academic Press.
- Jovičić, V. & Coop, M.R., 1998. The Measurement of Stiffness Anisotropy in Clays with Bender Element Tests in the Triaxial Apparatus. *Geotechnical Testing Journal*, 21, pp. 3-10. <https://doi.org/10.1520/GTJ10419J>
- Laloui, L., 2001. Thermo-mechanical behaviour of soils. *Revue Française de Génie Civil*, 5, pp. 809-843. <https://doi.org/10.1080/12795119.2001.9692328>
- Lourenço, S.D.N., Gallipoli, D., Augarde, C.E., Toll, D.G., Fisher, P.C. & Congreve, A., 2012. Formation and evolution of water menisci in unsaturated granular media. *Géotechnique*, 62, pp. 193-199. <http://dx.doi.org/10.1680/geot.11.P.034>
- Mancuso, C., Vassallo, R. & D'Onofrio, A., 2002. Small strain behavior of a silty sand in controlled-suction resonant column - torsional shear tests. *Canadian Geotechnical Journal*, 39(1), pp. 22-31. <https://doi.org/10.1139/t01-076>
- Ng, C.W.W., Akinniyi, D.B., Zhou, C. & Chiu, C.F., 2019. Comparisons of weathered lateritic, granitic and volcanic soils: Compressibility and shear strength. *Engineering Geology*, 249, pp. 235-240. <https://doi.org/10.1016/j.enggeo.2018.12.029>
- Ng, C.W.W. & Xu, J., 2012. Effects of current suction ratio and recent suction history on small-strain behaviour of an unsaturated soil. *Canadian Geotechnical Journal*, 49(2), pp. 226-243. <https://doi.org/10.1139/t11-097>
- Ng, C.W.W., Xu, J. & Yung, S.Y., 2009. Effects of wetting-drying and stress ratio on anisotropic stiffness of an unsaturated soil at very small strains. *Canadian Geotechnical Journal*, 46(9), pp. 1062-1076. <https://doi.org/10.1139/T09-043>
- Ng, C.W.W. & Yung, S.Y., 2008. Determination of the anisotropic shear stiffness of an unsaturated decomposed soil. *Géotechnique*, 58(1), pp. 23-35. <https://doi.org/10.1680/geot.2008.58.1.23>
- Ng, C.W.W. & Zhou, C., 2014. Cyclic behaviour of an unsaturated silt at various suctions and temperatures. *Géotechnique*, 64(9), pp. 709-720. <https://doi.org/10.1680/geot.14.P.015>
- Sawangsurriya, A., Edil, T.B. & Bosscher, P.J., 2009. Modulus-Suction-Moisture Relationship for Compacted Soils in Postcompaction State. *Journal of Geotechnical and Geoenvironmental*

Engineering (ASCE), 135(10), pp. 1390-1403. [https://doi.org/10.1061/\(ASCE\)GT.1943-5606.0000108](https://doi.org/10.1061/(ASCE)GT.1943-5606.0000108)

Thota, S.K. & Vahedifard, F., 2021. Stability analysis of unsaturated slopes under elevated temperatures. *Engineering Geology*, 293, 106317. <https://doi.org/10.1016/j.enggeo.2021.106317>

Uchaipichat, A. & Khalili, N., 2009. Experimental investigation of thermo-hydro-mechanical behaviour of an unsaturated silt. *Géotechnique*, 59(4), pp. 339-353. <https://doi.org/10.1680/geot.2009.59.4.339>

Vahedifard, F., Thota, S.K., Cao, T.D., Samarakoon, R.A. & McCartney, J.S., 2020. Temperature-Dependent Model for Small-Strain Shear Modulus of Unsaturated Soils. *Journal of Geotechnical and Geoenvironmental Engineering* (ASCE), 146(12). [https://doi.org/10.1061/\(ASCE\)GT.1943-5606.0002406](https://doi.org/10.1061/(ASCE)GT.1943-5606.0002406)

Wheeler, S.J. & Karube, D., 1996. State of the Art Report-Constitutive modelling. *Proceedings 1st International Conference on Unsaturated Soils*, Paris.

- This page is intentionally left blank -